cmgh
CELLULAR AND MOLECULAR GASTROENTEROLOGY AND HEPATOLOGY

ORIGINAL RESEARCH

Generation of Human iPSC–Derived Intestinal Epithelial Cell Monolayers by CDX2 Transduction

Kazuo Takayama,[1,2,3,4,*] Ryosuke Negoro,[1,*] Tomoki Yamashita,[1] Kanae Kawai,[4] Moe Ichikawa,[4] Takanori Mori,[5] Noriyuki Nakatsu,[6] Kazuo Harada,[7] Sumito Ito,[8] Hiroshi Yamada,[6] Yoshiyuki Yamaura,[5] Kazumasa Hirata,[7] Seiichi Ishida,[9] and Hiroyuki Mizuguchi[1,3,4,10]

[1]*Laboratory of Biochemistry and Molecular Biology, Graduate School of Pharmaceutical Sciences, Osaka University, Osaka, Japan;* [2]*PRESTO, Japan Science and Technology Agency, Saitama, Japan;* [3]*Laboratory of Hepatocyte Regulation, National Institutes of Biomedical Innovation, Health and Nutrition, Osaka, Japan;* [4]*Laboratory of Biochemistry and Molecular Biology, School of Pharmaceutical Sciences, Osaka University, Osaka, Japan;* [5]*Pharmacokinetic Research Laboratories, Ono Pharmaceutical Co, Ltd, Osaka, Japan;* [6]*Toxicogenomics Informatics Project, National Institutes of Biomedical Innovation, Health and Nutrition, Osaka, Japan;* [7]*Laboratory of Applied Environmental Biology, Graduate School of Pharmaceutical Sciences, Osaka University, Osaka, Japan;* [8]*GenoMembrane Co, Ltd, Kanagawa, Japan;* [9]*Division of Pharmacology, National Institute of Health Sciences, Kanagawa, Japan;* [10]*Global Center for Medical Engineering and Informatics, Osaka University, Osaka, Japan*

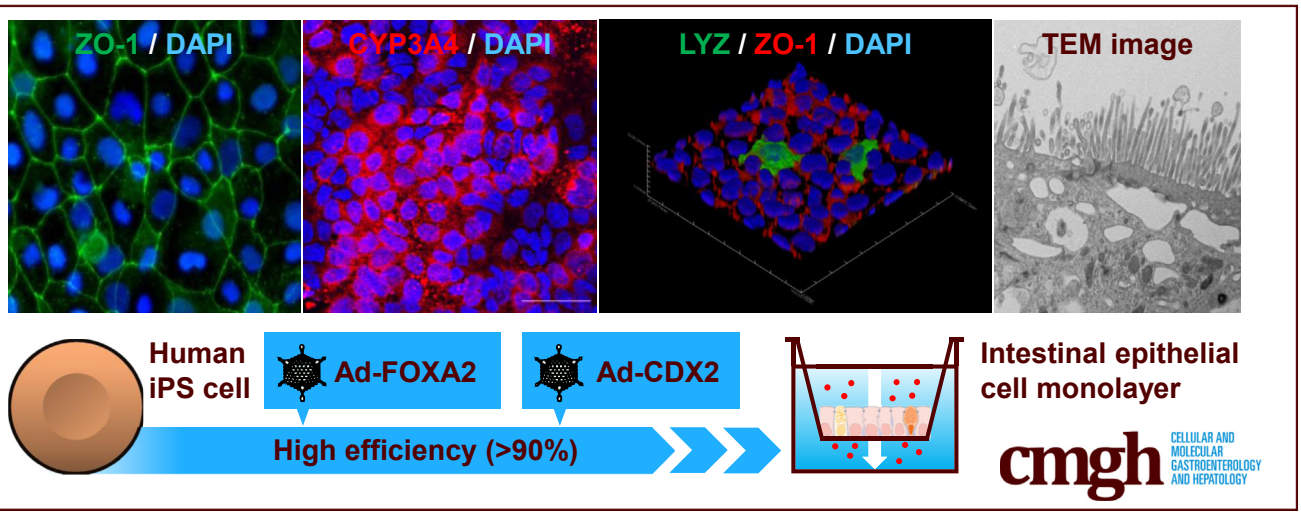

SUMMARY

We generated homogenous and functional intestinal epithelial cells from human induced pluripotent stem cells for pharmaceutical research by CDX2 transduction. Our human induced pluripotent stem cell–derived intestinal epithelial cell monolayers can predict intestinal absorption rate, intestinal first-pass effect, and drug-drug interactions of orally administered drugs.

BACKGROUND & AIMS: To develop an effective and safe orally administered drug, it is important to predict its intestinal absorption rate, intestinal first-pass effect, and drug-drug interactions of orally administered drugs. However, there is no existing model to comprehensively predict the intestinal pharmacokinetics and drug-response of orally administered drugs. In this study, we attempted to generate homogenous and functional intestinal epithelial cells from human induced pluripotent stem (iPS) cells for pharmaceutical research.

METHODS: We generated almost-homogenous Villin- and zonula occludens-1 (ZO1)-positive intestinal epithelial cells by caudal-related homeobox transcription factor 2 (CDX2) transduction into human iPS cell-derived intestinal progenitor cells.

RESULTS: The drug absorption rates in human iPS cell-derived intestinal epithelial cell monolayers (iPS-IECM) were highly correlated with those in humans (R^2=0.91). The expression levels of cytochrome P450 (CYP) 3A4, a dominant drug-metabolizing enzyme in the small intestine, in human iPS-IECM were similar to those in human small intestine *in vivo*. In addition, intestinal availability in human iPS-IECM (the fraction passing the gut wall: Fg=0.73) was more similar to that in the human small intestine *in vivo* (Fg=0.57) than to that in Caco-2 cells (Fg=0.99), a human colorectal adenocarcinoma cell line. Moreover, the drug-drug interaction and drug-food interaction could be observed by using our human iPS-IECM

in the presence of an inducer and inhibitor of CYP3A4, i.e., rifampicin and grape fruit juice, respectively.

CONCLUSION: Taking these results together, we succeeded in generating the human iPS-IECM that can be applied to various intestinal pharmacokinetics and drug-response tests of orally administered drugs. *(Cell Mol Gastroenterol Hepatol 2019;8:513–526; https://doi.org/10.1016/j.jcmgh.2019.06.004)*

Keywords: CYP3A4; Intestinal First-Pass Effect; Differentiation; Adenovirus.

The majority of orally administered drug absorption occurs at the human small intestine. Because the human small intestine expresses high levels of cytochrome P450 3A4 (CYP3A4) and other drug-metabolizing enzymes,[1,2] it plays an important role in not only drug absorption, but also drug metabolism. It is known that the intestinal first-pass metabolism of many clinically important CYP3A4 substrates contributes to their low oral bioavailability.[3] In addition, clinically important drug-drug interactions can take place via CYP3A4 induction or inhibition, as seen with verapamil and rifampicin (RIF)[4] and with cyclosporine and ketoconazole.[5] Such drug-drug interactions may cause unexpected side effects or reductions in drug efficacy. Therefore, it is essential to predict the intestinal absorption (the fraction absorbed [*Fa*]), intestinal first-pass effect (the fraction passing the gut wall [*Fg*]), and drug-drug interactions to develop safe and effective orally administered drugs. To date, however, no comprehensive system has been established for the prediction of intestinal pharmacokinetics and drug responses.

Because primary human intestinal epithelial cells are difficult to obtain and culture, experimental animals, Ussing chambers, and cancer cell lines are widely used as intestinal models for intestinal pharmacokinetics study. However, there are large species differences in drug metabolism between human and experimental animals such as mice and rats.[6] Although Ussing chambers and Caco-2 cells are good models for the evaluation of drug absorption, they cannot be utilized in drug metabolism and drug-drug interaction studies because they lack or underexpress the drug-metabolizing enzymes (eg, CYP3A4) as compared with the human adult small intestine in vivo.[7,8] In addition to the models mentioned previously, recent studies have shown that human intestinal epithelial cells could be generated from human embryonic stem cells, human induced pluripotent stem cells (iPSCs), human intestinal biopsies, and human fibroblasts.[9–15] Nonetheless, the CYP3A4 expression level was extremely low in human iPSC–derived intestinal epithelial cells (iPS-IECs) (approximately 1/100–1/1000 of the expression in the human adult small intestine in vivo).[9,16–18] Therefore, the previously developed human iPS-IECs, like Ussing chambers and Caco-2 cells, currently cannot be used for drug metabolism and drug-drug interaction studies. The method for differentiating intestinal epithelial cells must be improved to allow the use of human iPS-IECs for the prediction of fraction passing the gut wall (*Fg*), and drug-drug interactions.

To promote the differentiation of cells such as hepatocytes, osteoblasts, and adipocytes differentiations, we have demonstrated the effectiveness of gene transfer technologies using our fiber-modified adenovirus (AdK7) vector,[19] which contains a stretch of lysine residue (K7) peptides in the C-terminal region of the fiber knob for highly efficient transduction of human iPSCs and their derivatives, realizing a transfection efficiency of almost 100%.[20] Because many transcription factors are transiently expressed in the cellular differentiation process, we considered that vectors, such as adenovirus (Ad) vectors that can perform transient overexpression, are more suitable for cellular differentiation than lentivirus and retrovirus vectors. Previously, we succeeded in generating almost homogenous and highly functional hepatocyte-like cells from human iPSCs by AdK7 vector-mediated FOXA2, HNF1A, and HNF4A transductions.[20,21] Thus, in our present experiments, we tried to generate almost homogenous and highly functional intestinal epithelial cells from human iPSCs using AdK7 vector-based gene transfer technology.

For this purpose, we screened intestinal transcription factors to promote highly efficient intestinal differentiation from human iPSCs. Human iPSC–derived intestinal epithelial cell monolayers (iPS-IECMs) were generated on the chamber. We examined whether these monolayers could be used to evaluate the intestinal absorption rate, intestinal first-pass effect, and drug-drug interactions of orally administered drugs.

Results

Intestinal Differentiation Was Promoted by CDX2 Transduction

It is known that human iPSCs can differentiate into the intestinal epithelial cells via mesendoderm cells, definitive endoderm cells, and intestinal progenitor cells. To promote definitive endoderm differentiation, human iPSC–derived mesendoderm cells were transduced with FOXA2, as we have previously reported.[21] In this study, to improve the differentiation efficiency toward intestinal epithelial cells, we screened for intestinal transcription factors. Six

*Authors share co-first authorship.

Abbreviations used in this paper: **Ad-TF, transcription factor–expressing Ad vector; BIO, 6-Bromoindirubin-3′-oxime; CHGA, chromogranin A; *Fa*, fraction absorbed; FD-4, FITC-Dextran 4 kDa; *Fg*, fraction passing the gut wall; GAPDH, glyceraldehyde 3-phosphate dehydrogenase; GFJ, grapefruit juice; HBSS, Hank's Balanced Salt Solution; iPSC, induced pluripotent stem cell; IEC, intestinal epithelial cell; IECM, intestinal epithelial cell monolayer; LY, Lucifer yellow; LYZ, lysozyme; MDZ, midazolam; MRM, multiple-reaction monitoring; MUC2, mucin 2; Papp, apparent permeability coefficient; RIF, rifampicin; RT-PCR, reverse transcription-polymerase chain reaction; SI, sucrase isomerase; TEER, transepithelial electrical resistance; TF, transcription factor; UPLC-MS/MS, ultra-performance liquid chromatography tandem mass spectrometry, VD3, 1,25-dihydroxyvitamin D3; VP, vector particle; ZO-1, zonula occludens-1.**

Most current article

2352-345X
https://doi.org/10.1016/j.jcmgh.2019.06.004

candidate genes related to intestinal development were selected. Human iPSC–derived intestinal progenitor cells were transduced with transcription factor–expressing Ad vectors (Ad-TFs). The percentage of Villin+ and sucrose isomerase–positive (SI+) cells was significantly enhanced by Ad-CDX2 transduction (Villin+ = 93.2%, SI+ = 53.2%) (Figure 1*A*). These results suggest that intestinal differentiation could be promoted by CDX2 transduction. In addition, the gene expression levels of Villin, SI, intestine-specific homeobox, and CDX2 were increased by FOXA2 and CDX2 transductions (Figure 1*B*). The gene expression levels of intestinal transporters (peptide transporter 1, P-glycoprotein, breast cancer resistance protein) and drug-metabolizing enzyme CYP3A4 were also increased by FOXA2 and CDX2 transductions (Figure 1*C*). The percentages of Villin+ cells in Ad-LacZ–transduced cells and Ad-2TF–transduced cells were 38.9% and 96.2%, respectively (Figure 1*D*). These results suggest that highly efficient intestinal differentiation could be performed by sequential FOXA2 and CDX2 transduction. We also examined whether the expression of exogenous genes transduced by Ad vectors remain. The expression of exogenous CDX2 had almost disappeared at day 34 (Figure 1*E*). Instead, at day 34, the expression levels of endogenous CDX2 in the Ad-2TF–transduced cells were significantly higher than those of exogenous CDX2. This result suggests that the gene expression in the Ad-2TF–transduced cells is not influenced by the transgene at the end of intestinal differentiation. In addition, the gene expression levels of chromogranin A (CHGA), lysozyme (LYZ), and mucin 2 (MUC2) were increased during the intestinal differentiation. The procedure for intestinal differentiation is schematically presented in Figure 1*F*.

Human iPS-IECMs Have Drug Metabolism and Absorption Capacities

To examine whether the Ad-2TF–transduced cells have small intestinal or colonial characteristics, we performed a gene expression analysis of small intestine- and colon-specific markers (Figure 2). The gene expression profiles of the Ad-2TF–transduced cells were similar to those of the adult small intestine rather than the adult colon. This result suggests that the Ad-2TF–transduced cells resemble the adult small intestine rather than the adult colon.

The human iPS-IECMs generated on the chamber were positive for zonula occludens-1 (ZO1) and CYP3A4 (Figure 3*A*). We also performed an immunostaining analysis of CHGA, LYZ, and MUC2 to confirm the existence of enteroendocrine, Paneth, and goblet cells, respectively (Figure 3*B*). We confirmed the existence of other major intestinal epithelial cell types in our model. To examine the integrity of the human iPS-IECMs, we evaluated the barrier function of human iPS-IECMs. Barrier function in the human iPS-IECMs was analyzed by transepithelial electrical resistance (TEER) measurements, FD-4, and LY permeability tests. The TEER values in Ad-LacZ– and Ad-TF–transduced cells were approximately 420 $\Omega\times cm^2$ (Figure 4*A*). The FD-4 apparent permeability coefficient (Papp) values in Ad-LacZ– and Ad-TF–transduced cells were approximately 0.12×10^{-6} cm/s (Figure 4*B*). The FD-4 Papp values were increased by n-capric acid (C10, an absorption-enhancing agent) treatment. The Lucifer yellow (LY) Papp values in Ad-LacZ– and Ad-TF–transduced cells were approximately 0.44×10^{-6} cm/s (Figure 4*C*). The typical values of TEER (100–800 $\Omega\times cm^2$) and Papp ($<0.2–2\times10^{-6}$ cm/s) in Caco-2 cells are described in the guideline "Drug Interaction Studies–Study Design, Data Analysis, Implications for Dosing, and Labeling Recommendations" which was published by the Food and Drug Administration in 2006. These results suggest that human iPS-IECMs have an appropriate intestinal barrier function.

It is known that the drug-metabolizing enzyme CYP3A4 is strongly expressed in the human small intestine. Next, therefore, we examined the activities of CYP3A4 in human iPS-IECMs. The results showed that the CYP3A4 activities in Ad-TF–transduced cells were significantly higher than those in Ad-LacZ–transduced cells and Caco-2 cells (Figure 4*D*). In addition, the CYP3A4 induction potency was confirmed in both Ad-LacZ–transduced cells and Ad-TF–transduced cells (Figure 4*E*). These results suggest that human iPS-IECMs can be utilized in CYP3A4-mediated pharmacokinetic testing.

To further characterize the human iPS-IECMs, we performed global gene expression analysis in the human iPS-IECMs. The gene expression profiles of CYPs (Figure 5*A*) and adenosine triphosphate–binding cassette transporters (Figure 5*B*) in the human iPS-IECMs were similar to those in the human adult small intestine in vivo rather than Caco-2 cells. These results suggest that our human iPS-IECMs resemble to human adult small intestine rather than Caco-2 cells.

Human iPS-IECMs Can Be Utilized in Evaluating Fg and Predicting Drug-Drug Interaction

To examine whether the Ad-2TF–transduced iPS-IECMs can be applicable to drug permeability studies, apical to basolateral permeability of various drugs (antipyrine, metoprolol, fexofenadine, atenolol, and pravastatin) across the human iPS-IECMs was measured (Figure 6*A*). The Papp values of each drug in Ad-LacZ–transduced human iPS-IECMs, Ad-2TF–transduced iPS-IECMs, and Caco-2 cells highly correlated with *Fa* values in human in vivo (R^2 = 0.94, 0.91, and 0.97, respectively). To examine whether the human in vivo *Fg* can be predicted by human iPS-IECMs, the CYP3A4 substrate passing the human iPS-IECMs were evaluated by quantifying the midazolam (MDZ) and 1′-OH MDZ in apical chamber, basolateral chamber, and cells after 60-minute incubation (Figure 6*B*). The *Fg* value (*Fg* = 0.73) of human iPS-IECMs was similar to that of human intestinal tissue (*Fg* = 0.57) rather than Caco-2 cells (*Fg* = 0.99).

To examine whether the Ad-2TF–transduced iPS-IECMs can be utilized in drug-drug interaction and drug-food interaction studies, amiodarone-induced hepatotoxicity was evaluated in the presence of 1,25-dihydroxyvitamin D3 (VD3)/RIF (VD3 + RIF, CYP3A4 inducers) or grapefruit juice (GFJ) components (CYP3A4 inhibitors). The amiodarone-treated human iPS-IECMs were co-cultured with human iPSC–derived hepatocyte-like cells to detect

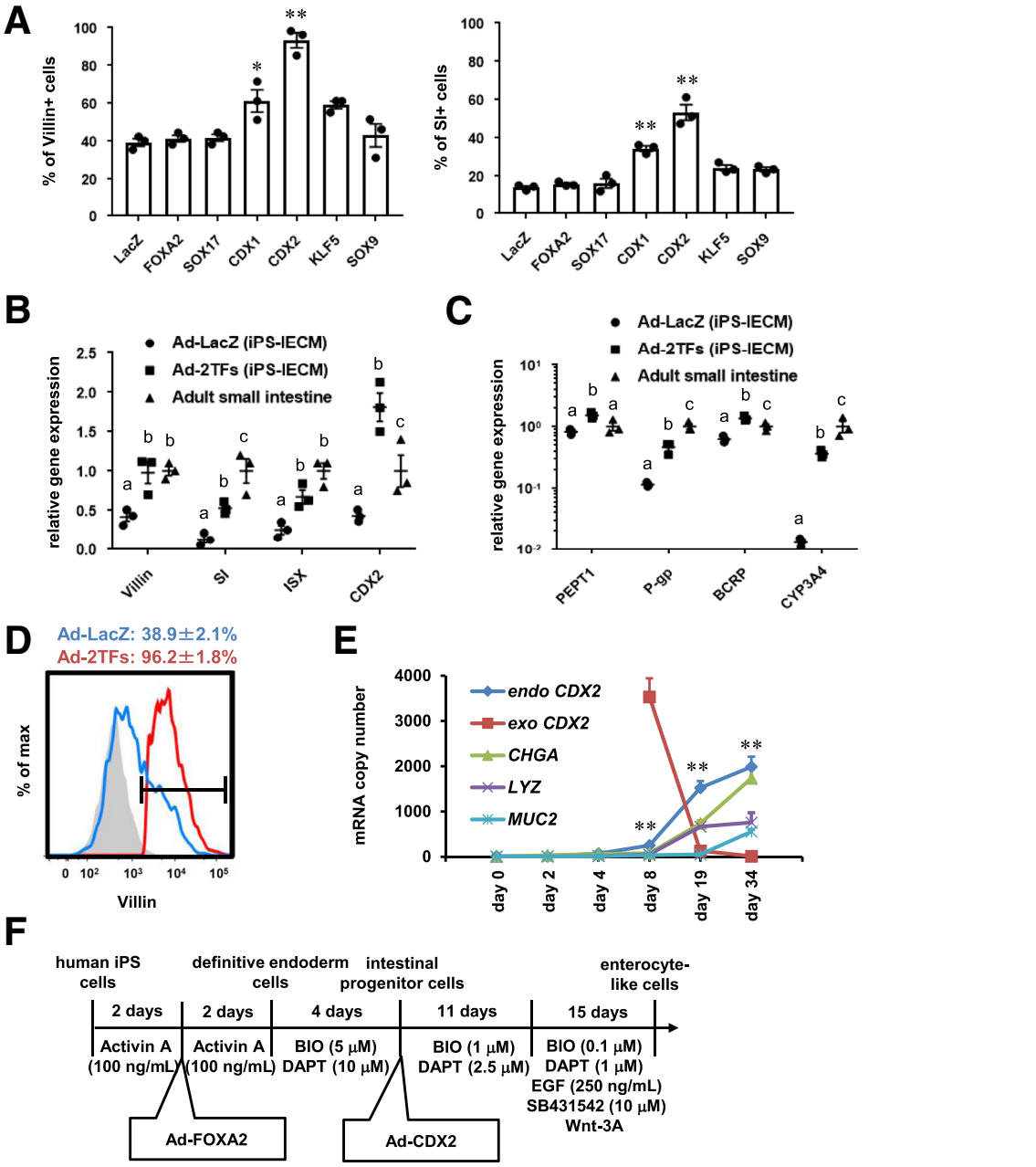

Figure 1. Intestinal differentiation was promoted by CDX2 transduction. (*A*) Human iPSCs were differentiated into the intestinal progenitor cells as described in the Materials and Methods section. At day 8 of the differentiation, the intestinal progenitor cells were transduced with 3000 VPs/cell of Ad-TFs for 1.5 hours. Ad-TF–transduced intestinal progenitor cells were differentiated into intestinal epithelial cells as described in the Materials and Methods section. At day 34 of the differentiation, the percentage of Villin+ (left) and SI+ (right) cells was examined by fluorescence-activated cell sorting (FACS) analysis. Statistical significance was evaluated by 1-way analysis of variance followed by Bonferroni's post hoc tests (*$P < .05$, **$P < .01$, vs Ad-LacZ–transduced cells). (*B*) The gene expression levels of Villin, SI, ISX, and CDX2 in Ad-LacZ–transduced cells, Ad-FOXA2-CDX2 (2TFs)–transduced cells, fetal small intestine, and adult small intestine were examined by real-time RT-PCR. The gene expression levels in the small intestine were taken as 1.0. (*C*) The gene expression levels of peptide transporter 1, P-glycoprotein, breast cancer resistance protein, and CYP3A4 in Ad-LacZ–transduced cells, Ad-FOXA2-CDX2 (2TFs)–transduced cells, fetal small intestine, and adult small intestine were examined by real-time RT-PCR. The gene expression levels in the small intestine were taken as 1.0. (*B*, *C*) Statistical significance was evaluated by 2-way analysis of variance followed by Tukey's post hoc tests. Groups that do not share the same letter are significantly different from each other ($P < .05$). (*D*) The percentage of Villin+ cells in Ad-LacZ–transduced cells and Ad-2TF–transduced cells was examined by FACS analysis. (*E*) The endogenous and exogenous CDX2, CHGA, LYZ, and MUC2 expression levels were measured by absolute real-time RT-PCR. Statistical significance was evaluated by Student's *t* test (endogenous CDX2 vs exogenous CDX2; **$P < .01$). (*F*) The procedure for intestinal differentiation is presented schematically. Details of the intestinal differentiation procedure are described in the Materials and Methods section. All data are shown as the mean ± SE of 3 independent differentiation experiments.

hepatotoxicity. Amiodarone is widely used, either intravenously or orally for arrhythmia treatment. It is also known that clinically apparent liver injury occurs in up to 1% of amiodarone-treated patients annually.[22] Amiodarone is known to be metabolized by CYP3A4 and its metabolites show hepatotoxicity.[23] In the presence of VD3/RIF (CYP3A4 inducers), amiodarone-induced hepatotoxicity was significantly increased (Figure 7*A*). The concentration of amiodarone metabolites in the basal chamber may have been increased because the CYP3A4 activity in human iPS-IECMs was increased by VD3/RIF. In the presence of the GFJ components (CYP3A4 inhibitors), amiodarone-induced hepatotoxicity was significantly decreased (Figure 7*B*). The concentration of amiodarone metabolites in the basal chamber may have been decreased because the CYP3A4 activity in human iPS-IECMs was decreased by the GFJ components. These results suggest that the human iPS-IECMs can be utilized in drug-drug interaction and drug-food interaction studies.

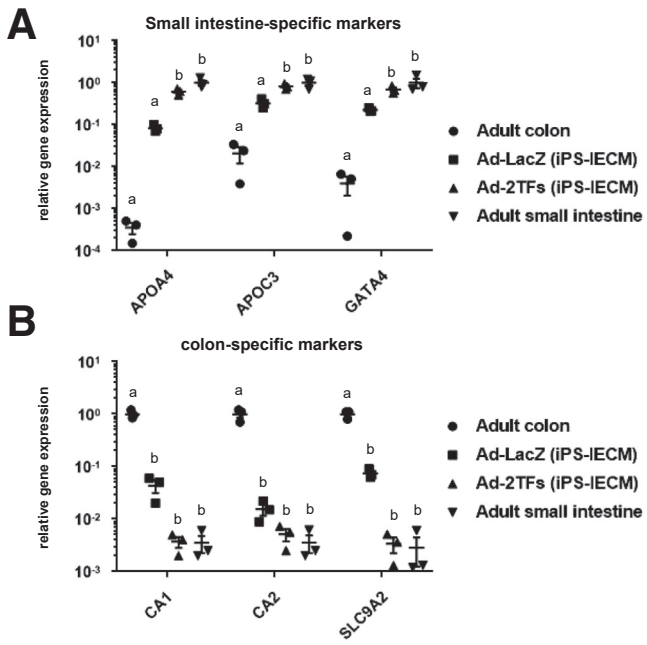

Figure 2. The gene expression analysis of small intestine- and colon-specific markers. Human iPSCs were differentiated into the intestinal epithelial cell monolayers as described in the Materials and Methods section. The gene expression levels of (*A*) small intestine-specific markers and (*B*) colon-specific markers in Ad-LacZ–transduced cells, Ad-FOXA2-CDX2 (2TFs)–transduced cells, adult colon, and adult small intestine were examined by real-time RT-PCR. The gene expression levels in (*A*) the adult small intestine and (*B*) adult colon were taken as 1.0. Statistical significance was evaluated by 2-way analysis of variance followed by Tukey's post hoc tests. Groups that do not share the same letter are significantly different from each other ($P < .05$). All data are shown as the mean ± SE of 3 independent differentiation experiments.

Discussion

In this study, almost homogenous and highly functioning human iPS-IECMs were generated from human iPSCs by CDX2 transduction. Our experiments showed that the human iPS-IECMs could be used to evaluate the intestinal absorption rate, intestinal first-pass effect, and drug-drug interactions of orally administered drugs.

The intestinal differentiation efficiency and expression levels of drug transporters and metabolizing enzymes were enhanced by CDX2 transduction. Although it was difficult to generate human iPS-IECs that had CYP3A4 expression levels as high as those in the human intestine in vivo,[9,16,18] the CYP3A4 expression levels in our Ad-2TF–transduced iPS-IECMs were closer to those in the human adult small intestine in vivo as compared with Ad-LacZ–transduced iPS-IECMs and Caco-2 cells. It is reported that the expression of Cdx2 is essential for the intestinal homeostasis and differentiation of gut stem cells into any of the intestinal cell types.[24,25] It is also known that Cdx2 ectopic expression induces gastric intestinal metaplasia and that overexpression of CDX2 in gastric cancer cells upregulates the expression of drug transporters.[26,27] Taken together, these results indicate that high expression of CDX2 is necessary for both intestinal differentiation and acquisition of intestinal functions. In the future, we would like to identify a small molecular compound capable of inducing CDX2 expression, to develop a simple and efficient intestinal differentiation method from human iPSCs.

Recently, Kasendra et al developed a human Small Intestine-on-a-Chip using biopsy-derived organoids and Caco-2 cells, which can evaluate radiation injury–induced cell death and drug responses.[28,29] To further mimic the complex physical and biochemical microenvironment of living human small intestine, Organ-on-Chip technologies, which can recapitulate the fluid flow and peristalsis-like motions of in vivo tissue, should be adopted in the future. If a 2-channel Organ-on-Chip device consisting of human iPS-IECMs and hepatocyte-like cells were developed, it could be used to predict oral bioavailability ($F = Fa \times Fg \times Fh$). We consider that the oral bioavailability of poor metabolizers (patients lacking the activity of a certain cytochrome P450) would be predicted by using Organ-on-Chip devices consisting of poor metabolizer-derived iPSCs, which we have established previously.[30]

Here, we developed the human iPS-IECMs, which can be used to evaluate the intestinal absorption rate, intestinal first-pass effect, and drug-drug interactions of orally administered drugs. To further characterize our human iPS-IECMs, we will need to accumulate more data on the absorption rate and intestinal first-pass effect by using other clinically important substrates. Because it is known than not only CYP3A4 but also CYP2C are expressed in the human adult small intestine *in vivo*, it would be possible to predict the intestinal first-pass effect of CYP2C substrates by using our model. Moreover, it might be possible to use our model to elucidate the mechanisms of clinically relevant drug-drug interactions and drug-induced liver and intestinal injuries. We believe that our human iPS-IECMs will be utilized in the early phase of pharmaceutical development, thereby helping to avoid failure in drug development due to

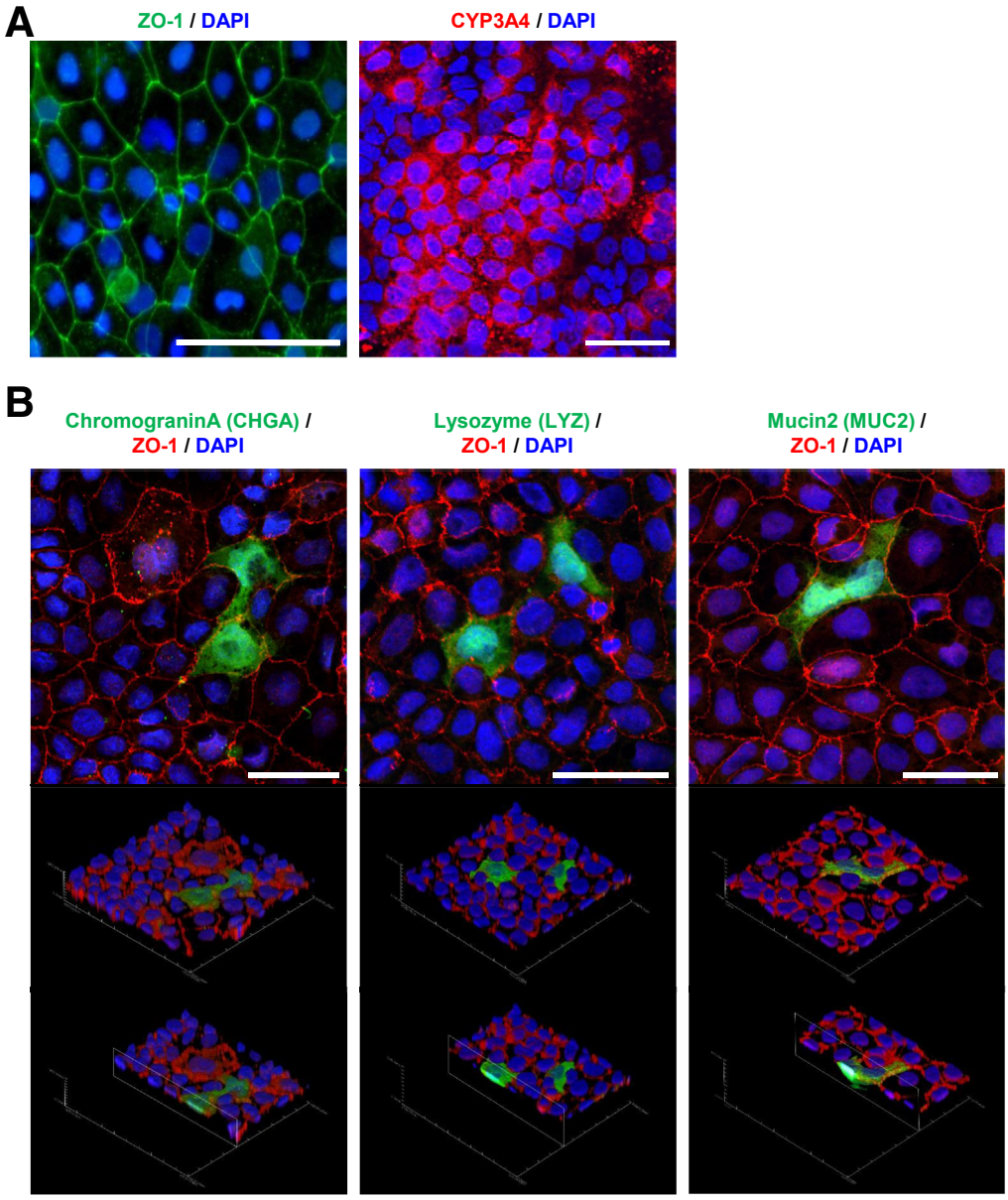

Figure 3. Immunostaining analysis of human iPS-IECMs. Human iPSCs were differentiated into the intestinal epithelial cell monolayers on the chamber as described in the Materials and Methods section. (*A*) The ZO-1 and CYP3A4 expression levels were examined by immunostaining analysis. Nuclei were counterstained with DAPI. Scale bars = 50 μm. (*B*) Immunostaining analysis of CHGA, LYZ, MUC2, and ZO-1 was performed in the human iPS-IECMs. Nuclei were stained with DAPI (blue). Scale bars = 50 μm.

pharmacokinetic/bioavailability failures and harmful drug-drug interactions.

Materials and Methods

Human iPSC Culture

The human iPSC line, YOW-iPSC,[30] was maintained on a feeder layer of mitomycin C-treated mouse embryonic fibroblasts (Millipore, Bedford, MA) with ReproStem medium (ReproCELL, Yokohama, Japan) supplemented with 10-ng/mL fibroblast growth factor 2 (Katayama Chemical Industries, Osaka, Japan).

In Vitro Intestinal Differentiation

Before the initiation of intestinal differentiation, human iPSCs were dissociated into clumps by using dispase (Roche Diagnostics, Indianapolis, IN) and plated onto the BD Matrigel Matrix Growth Factor Reduced–coated apical chamber (BD Biosciences, San Jose, CA) of BD Falcon cell culture inserts (6-well plate, 1.0-μm pore size, 1.6 $\times$ 10^6 pores/cm; PET Membrane). These cells were cultured in the mouse embryonic fibroblast–conditioned medium for 2–3 days. The differentiation protocol for the induction of definitive endoderm cells was described previously.[9,16] Briefly, for the definitive endoderm differentiation, human iPSCs were cultured for 4 days in RPMI1640 medium (Sigma- Aldrich, St. Louis, MO) containing 100 ng/mL Activin A (R&D Systems, Minneapolis, MN), 1$\times$GlutaMAX (Thermo Fisher Scientific, San Jose, CA), penicillin-streptomycin, and 1$\times$B27 Supplement Minus Vitamin A (Thermo Fisher Scientific). During the definitive endoderm differentiation, the mesendoderm cells (day 2) were transduced with 3000 VPs/cell of Ad-FOXA2 for 1.5 hours to promote definitive endoderm differentiation.

For the induction of intestinal progenitor cells, the definitive endoderm cells were cultured for 4 days in the intestinal differentiation medium (Dulbecco's modified Eagle medium, high glucose [FUJIFILM Wako, Osaka, Japan])

containing 5-μM 6-Bromoindirubin-3′-oxime (BIO) (Calbiochem, San Diego, CA), 1×MEM Non-Essential Amino Acids Solution (Thermo Fisher Scientific), Penicillin-Streptomycin, 1×GlutaMAX, and 100 μM β-mercaptoethanol. supplemented with 10 μM N-[(3,5-difluorophenyl) acetyl]-L-alanyl-2-phenyl-1, 1-dimethylethyl ester-glycine (DAPT) (Peptide Institute, Osaka, Japan), and 10% Knockout Serum Replacement (Thermo Fisher Scientific).

For the induction of intestinal epithelial cell monolayers, the intestinal progenitor cells were cultured for 11 days in

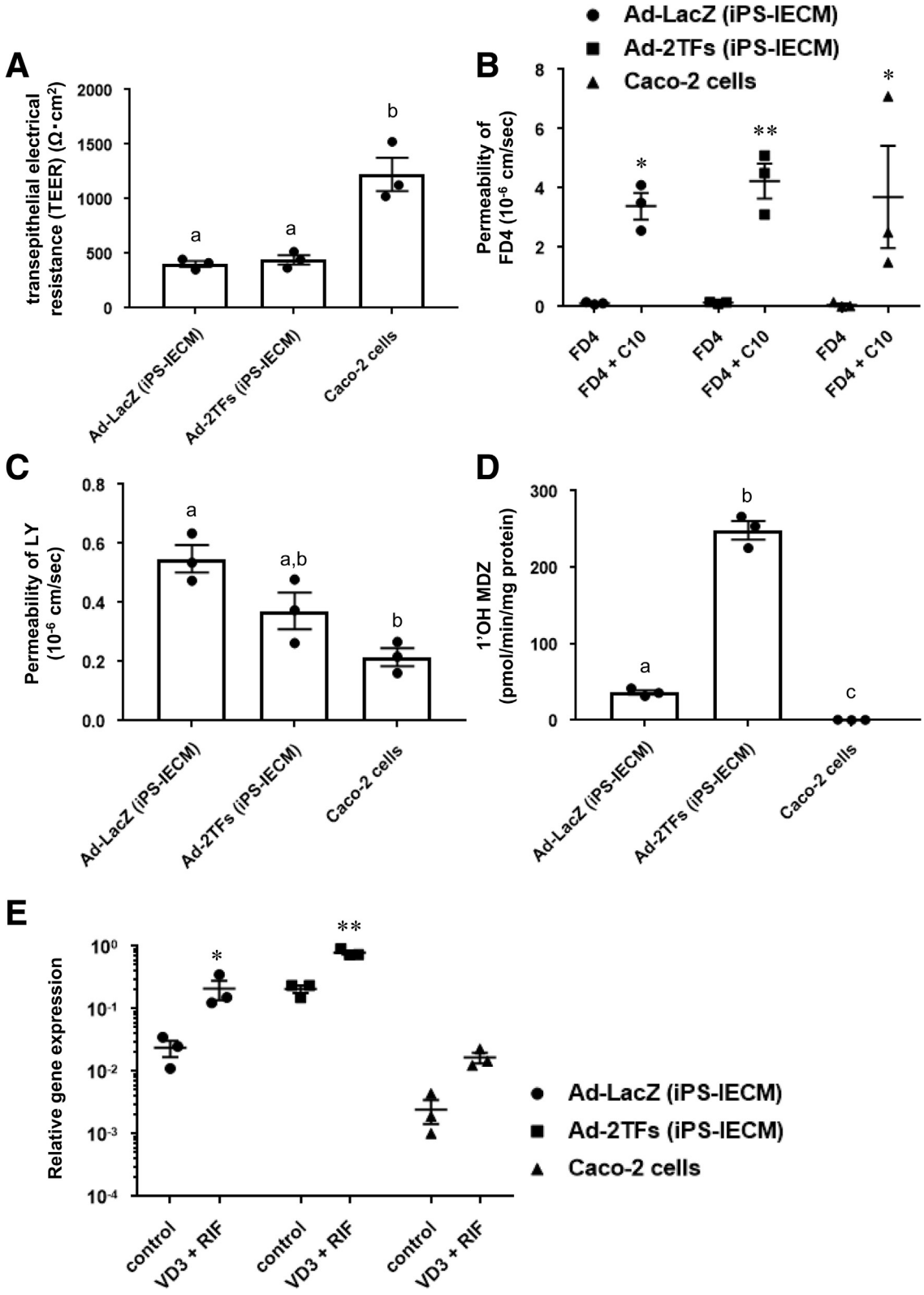

intestinal differentiation medium supplemented with 1-μM BIO and 2.5-μM DAPT, and then cultured for 15 days in the Wnt-3A–conditioned intestinal differentiation medium supplemented with 0.1-μM BIO, 1-μM DAPT, 250-ng/mL epidermal growth factor, and 10 μM SB431542. During the intestinal differentiation, the intestinal progenitor cells (day 8) were transduced with 3000 VPs/cell of Ad-CDX2 for 1.5 hours to promote intestinal differentiation.

Caco-2 Cell Culture and Differentiation

The human colorectal adenocarcinoma cell line, Caco-2 (HTB-37), was obtained from the American Type Culture Collection (ATCC, Rockville, MD). Caco-2 cells were cultured with Dulbecco's modified Eagle medium, high glucose containing 1×HEPES (Thermo Fisher Scientific), 10% fetal bovine serum, 1×MEM Non-Essential Amino Acids Solution, penicillin-streptomycin, and 1×GlutaMAX. For differentiation of Caco-2 cells, Caco-2 cells were cultured for 21 days after they reached confluence. The passage number of the Caco-2 cells was between 20 and 40.

RNA Isolation and Reverse-Transcription Polymerase Chain Reaction

Total RNA was isolated from Caco-2 cells, human iPSC–derived cells using ISOGENE (NIPPON GENE, Tokyo, Japan). Total RNA of Human Adult Normal Tissue 5 Donor Pool: Small Intestine and Human Adult Normal Tissue: Colon was purchased from BioChain Institute. Complementary DNA was synthesized using 500 ng of total RNA with a Superscript VILO complementary DNA synthesis kit (Thermo Fisher Scientific). Real-time reverse-transcription polymerase chain reaction (RT-PCR) was performed with SYBR Green PCR Master Mix (Applied Biosystems, Foster City, CA) using a StepOnePlus real-time PCR system (Applied Biosystems). The relative quantitation of target messenger RNA levels was performed by using the $2^{-\Delta\Delta CT}$ method. The values were normalized by those of the housekeeping gene, glyceraldehyde 3-phosphate dehydrogenase (GAPDH). PCR primer sequences were obtained from PrimerBank (https://pga.mgh.harvard.edu/primerbank/).

Immunohistochemistry

To perform the immunohistochemistry, the human iPSC–derived cells were fixed with 4% paraformaldehyde in phosphate-buffered saline for 10 minutes. After blocking the cells with phosphate-buffered saline containing 10% fetal bovine serum, 1% bovine serum albumin, and 1% Triton X-100 for 45 minutes, the cells were incubated with anti-human ZO-1 antibodies (sc10804), anti-human CYP3A4 antibodies (sc-27639), anti-human CHGA antibodies (ab80787), anti-human MUC2 antibodies (ab118964), or anti-human LYZ (ab36362) at 4°C overnight, and finally, incubated with Alexa Fluor 488– or 594–labeled secondary antibodies (Thermo Fisher Scientific) at room temperature for 1 hour. Images were taken with a fluorescence microscope (Biozero BZ-9000; KEYENCE, Osaka, Japan) or a confocal laser scanning microscope (FLUOVIEW FV10i; Olympus Life Science, Tokyo, Japan).

Flow Cytometry

Single-cell suspensions of the human iPSC–derived cells were treated with 1×Permeabilization Buffer (e-Bioscience, San Diego, CA), and then incubated with anti-human Villin antibodies (ab109516) or anti-human Sucrase Isomaltase antibodies (sc27603), followed by Alexa Fluor 488–labeled secondary antibodies (Thermo Fisher Scientific). Analysis was performed on a MACSQuant Analyzer (Miltenyi Biotec, Bergisch Gladbach, Germany) and FlowJo software (FlowJo LLC, BD Biosciences).

CYP3A4 Activity

In Figure 4*D*, ultra-performance liquid chromatography tandem mass spectrometry (UPLC-MS/MS) analysis was performed to examine the CYP3A4 activity. Human iPSC–derived cells and Caco-2 cells were cultured with medium containing 5-μM MDZ (FUJIFILM Wako). The metabolites of each substrate are 1′-OH MDZ. After the treatment with substrates, the supernatant was collected at 2 hours, and then immediately mixed with 2 volumes of acetonitrile (FUJIFILM Wako). Samples were filtrated with AcroPrep Advance 96-well Filter Plates (Pall Corporation, Port Washington, NY) for 5 minutes at 1750 *g*, and then the supernatant was analyzed by UPLC-MS/MS to measure the concentration of metabolites according to each standard curve. UPLC analysis was performed using an Acquity UPLC (Waters, Milford, MA) and MS/MS was performed on a Q-Premier XE (Waters). The mass spectrometer was set to the multiple-reaction monitoring (MRM) mode and was operated with

Figure 4. (***See previous page***). **Barrier and metabolic functions of human iPSC–derived intestinal epithelial cell monolayers.** (*A*) TEER values of the Ad-LacZ–transduced iPS-IECMs, Ad-2TF–transduced iPS-IECMs, and Caco-2 monolayers were measured by Millicell-ERS2. (*B*) Apical-to-basolateral permeability of FD4 across the Ad-LacZ–transduced monolayers, Ad-2TF–transduced monolayers, and Caco-2 monolayers was measured in the presence or absence of C10 (an absorption-enhancing agent). (*C*) Apical-to-basolateral permeability of LY across the Ad-LacZ–transduced iPS-IECMs, Ad-2TF–transduced iPS-IECMs, and Caco-2 monolayers was measured. (*D*) The CYP3A4-mediated drug metabolizing capacities in the Ad-LacZ–transduced iPS-IECMs, Ad-2TF–transduced iPS-IECMs, and Caco-2 monolayers were evaluated by quantifying the metabolites of the CYP3A4 substrate, MDZ. The quantity of metabolites, 1′-OH MDZ, was measured by UPLC-MS/MS. (*E*) To examine CYP3A4 induction potency, the cells were treated with 100-nM VD3 for 21 days and 20-μM RIF for 2 days. The gene expression levels of *CYP3A4* were measured by real-time RT-PCR. Controls were treated with DMSO (final concentration 0.1%). The gene expression levels in the human small intestine were taken as 1.0. (*A*, *C*, *D*) Statistical significance was evaluated by 1-way analysis of variance followed by Tukey's post hoc tests. Groups that do not share the same letter are significantly different from each other ($P < .05$). (*B*, *E*) Statistical significance was evaluated by 2-way analysis of variance followed by Bonferroni's post hoc tests (*$P < .05$, **$P < .01$, FD4 vs FD4 + C10 and control vs VD3 + RIF, respectively). The results are shown as the mean ± SE of 3 independent differentiation experiments.

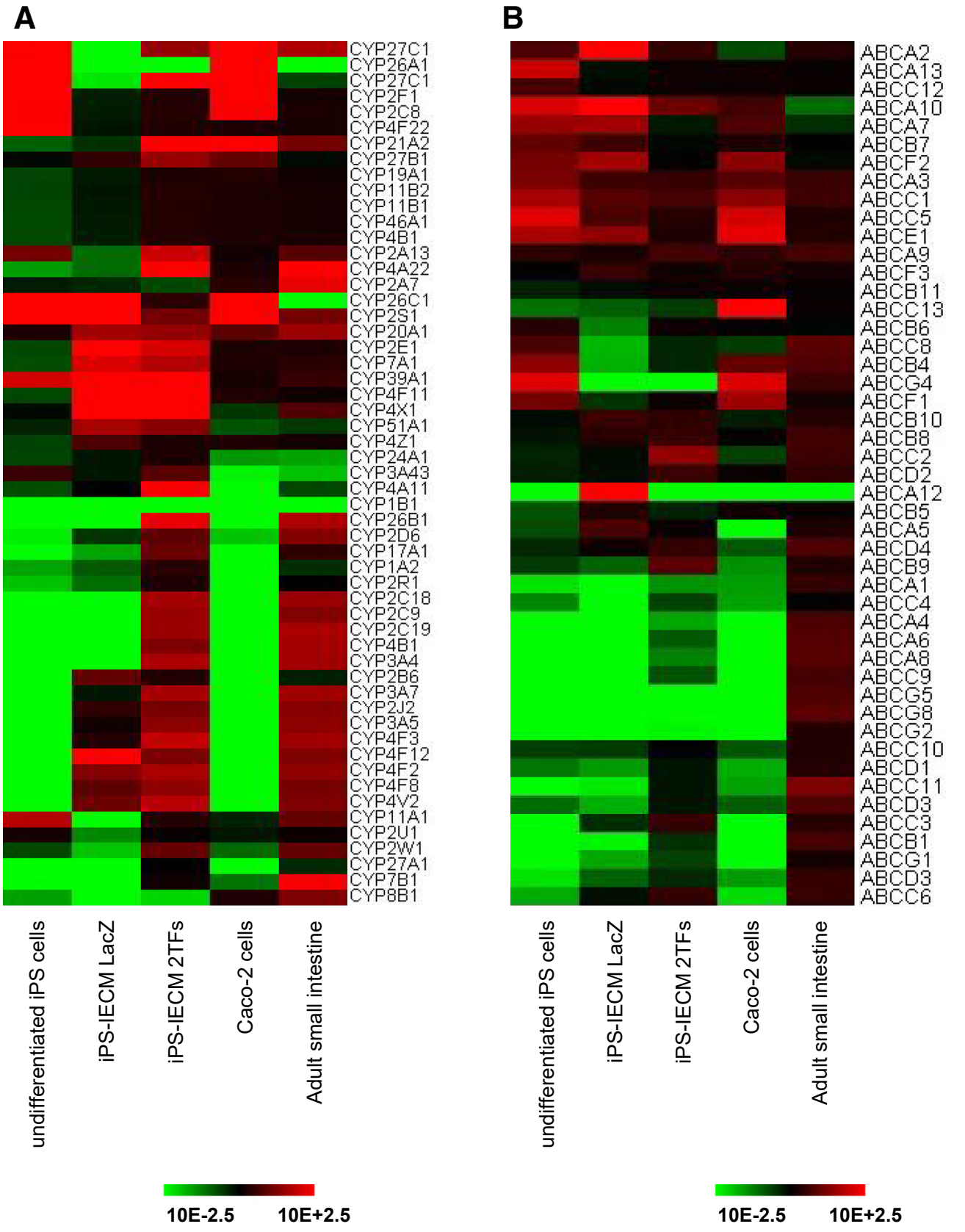

Figure 5. The gene expression profile of CYPs and ABC transporters in human iPS-IECMs. Human iPSCs were differentiated into the intestinal epithelial cell monolayers as described in the Materials and Methods section. The global gene expression analysis was performed in undifferentiated human iPSCs, human Ad-LacZ–transduced iPS-IECMs, human Ad-2TF–transduced iPS-IECMs, Caco-2 cells, and the human adult small intestine in vivo. Heatmap analyses of (*A*) CYPs and (*B*) ABC transporters are shown.

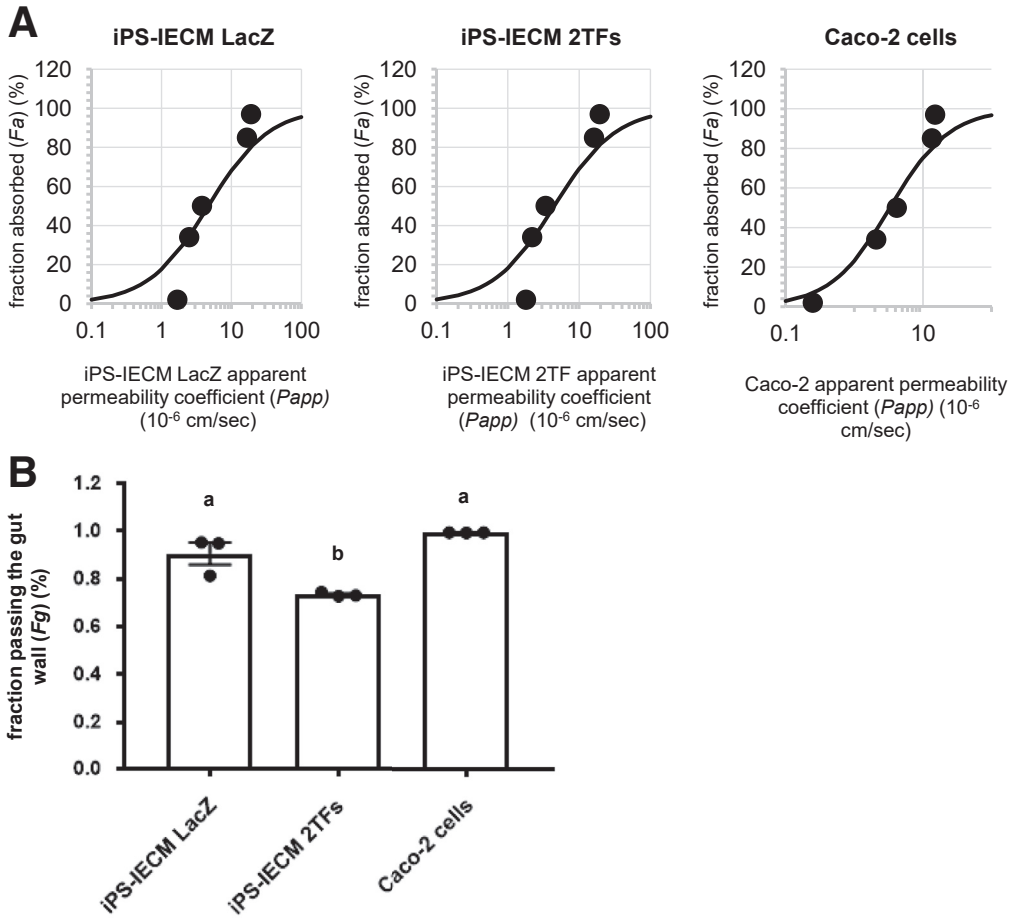

Figure 6. Human iPSC–derived intestinal epithelial cell monolayers can be utilized in evaluating *Fg* value. Human iPSCs were differentiated into the intestinal epithelial cell monolayers on the chamber as described in the Materials and Methods section. (*A*) The apical-to-basolateral permeability of antipyrine, metoprolol, fexofenadine, atenolol, and pravastatin across the Ad-2TF–transduced iPS-IECMs was measured. The data on the human proximal jejunum permeability of antipyrine, metoprolol, fexofenadine, atenolol, and pravastatin in vivo are cited from previously published papers.[35–37] (*B*) To examine the in vitro *Fg* in the Ad-LacZ– and Ad-2TF–transduced iPS-IECMs and Caco-2 cells, the CYP3A4-mediated drug metabolizing capacities were evaluated by quantifying the MDZ and 1′-OH MDZ in the apical chamber, basolateral chamber, and cells. The *Fg* was calculated as described in the Materials and Methods section. Statistical significance was evaluated by 1-way analysis of variance followed by Tukey's post hoc tests. Groups that do not share the same letter are significantly different from each other ($P < .05$). The results are shown as the mean ± SE of 3 independent differentiation experiments.

the electrospray ionization source in positive ion mode. MRM transition (*m/z* of precursor ion / *m/z* of product ion) for 1′-OH MDZ were 342.2/203.1. For transition, the cone voltage and collision energy were set at 40 V and 26 eV, respectively. The dwell time for each MRM transition was set at 100 ms. LC separations were carried out at 40°C with an Acquity UPLC BEH C18 column, 1.7 μm, 2.1 × 50 mm (Waters). The mobile phase was delivered at a flow rate of 0.5 mL/min using a gradient elution profile consisting of solvent A (0.1% formic acid/distilled water) and solvent B (acetonitrile). The initial composition of the binary solvent was 10% B from 0 to 0.5 minutes. Solvent B was increased from 10% to 100% over 2.0 minutes. The composition of solvent remained for 1.0 minutes at 100% B. Ten microliters of sample solution was injected into the column. The concentrations of each metabolite were calculated according to each standard followed by normalization to the protein content per well.

CYP3A4 Induction

Total RNA was isolated using an RNeasy Mini Kit (QIAGEN, Hilden, Germany). To measure CYP3A4 induction potencies, the gene expression levels of *CYP3A4* were measured by real-time RT-PCR. Real-time RT-PCR was performed with TaqMan Gene Expression Assays (Applied Biosystems). The assay ID for CYP3A4 is Hs00430021_m1 (Applied Biosystems). The cells were treated with 100 nM VD3 (Sigma-Aldrich) for 21 days and 20 μM RIF (FUJIFILM Wako) for 2 days; these agents are known to induce CYP3A4. Controls were treated with dimethyl sulfoxide (final concentration 0.1%; FUJIFILM Wako). Inducer compounds were replaced daily. Relative quantification was performed against a standard curve and the values were normalized against the input determined for the housekeeping gene, GAPDH, and beta-actin. The assay IDs for GAPDH and beta-actin are Hs02758991_g1 and Hs01060665_g1 (all from Applied Biosystems), respectively.

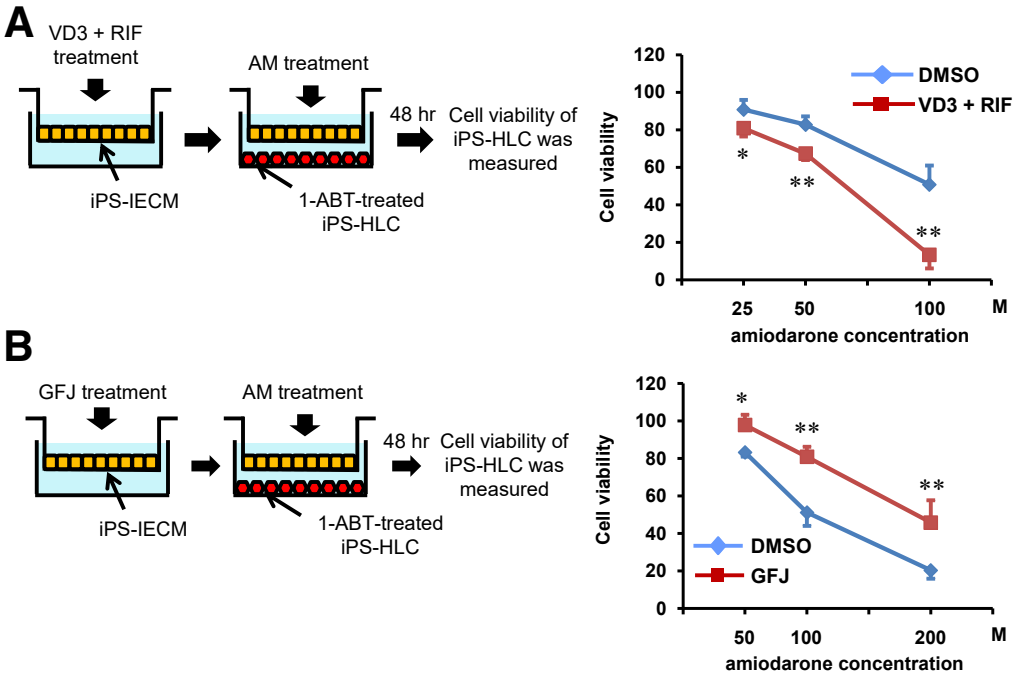

Figure 7. Human iPSC–derived intestinal epithelial cell monolayers can be utilized in predicting drug-drug interactions. Human iPSCs were differentiated into the intestinal epithelial cell monolayers on the chamber as described in the Materials and Methods section. (*A*) To induce CYP3A4 activity, Ad-2TF–transduced iPS-IECMs were cultured with VD3 for 21 days and RIF for 2 days. Ad-2TF–transduced iPS-IECMs and 1-aminobenzotriazole–treated iPSC-derived hepatocyte-like cells were co-cultured with amiodarone-containing medium for 48 hours. The cell viability of the hepatocyte-like cells was measured. The cell viability of nontreated cells was taken as 100. Statistical significance was evaluated by repeated 2-way analysis of variance followed by Bonferroni's post hoc tests (*$P < .05$, **$P < .01$, DMSO vs VD3 + RIF). (*B*) To inhibit CYP3A4 activity, Ad-2TF–transduced iPS-IECMs were cultured with 6′,7′-dihydroxybergamottin and bergamottin (GFJ) for 48 hours. Ad-2TF–transduced iPS-IECMs and hepatocyte-like cells were co-cultured with Amiodarone-containing medium for 48 hour. The cell viability of the hepatocyte-like cells was measured. The cell viability of nontreated cells was taken as 100. Statistical significance was evaluated by repeated 2-way analysis of variance followed by Bonferroni's post hoc tests (*$P < .05$, **$P < .01$, DMSO vs GFJ). The results are shown as the mean ± SE of 3 independent differentiation experiments.

TEER Measurements

TEER of human iPSC–derived cells and Caco-2 cells, which were cultured on BD Falcon cell culture inserts (6-well plate, 1-μm pore size, 1.6×10^6 pores/cm^2; BD Biosciences) from day 0 of differentiation, was measured by Millicell-ERS2 (Merk Millipore). The raw data were converted to $\Omega \times$cm^2 based on the culture insert area (4.2 cm^2).

Calculation of Apparent Permeability

The *Papp* in transport assay was calculated according to the following equation.

$$Papp = \delta Cr / \delta t \times Vr / (A \times C_0)$$

$\delta Cr / \delta t$ = permeability rate (δCr = final receiver concentration, δt = assay time); Vr = receiver volume; A = transwell growth area; C_0 = initial concentration in the donor compartment.

FD-4 Permeability Tests

Human iPSC–derived cells and Caco-2 cells, which were cultured on the cell culture inserts, were rinsed with Hank's Balanced Salt Solution (HBSS). The 2 mL of HBSS containing 10-mg/mL FD-4 (average molecular weight 3000–5000; Sigma-Aldrich) with or without 13-mM n-capric acid (C10; Nacalai tesque, Kyoto, JAPAN) was added to the apical chamber, and 2.9 mL of HBSS was added to the basolateral chamber. Ca^{++}/Mg^{++}-free HBSS (Thermo Fisher Scientific) was used in the apical chamber to avoid precipitation of C10. Exclusion of Ca^{++}/Mg^{++} from the apical solutions did not affect the integrity of the monolayers because the HBSS in the basolateral chamber contained Ca^{++}/Mg^{++}. After 90 minutes of incubation at 37°C, the solution was collected from the basolateral side. The FD-4 fluorescent signal was measured with a fluorescence plate reader (TriStar LB 941; Berthold Technologies, Bad Wildbad, Germany) using 490-nm excitation and 520-nm emission filters. FD-4 concentrations were calculated using the standard curve generated by serial dilution of FD-4.

LY Permeability Tests

Human iPSC–derived cells and Caco-2 cells, which were cultured on the cell culture inserts, were rinsed with HBSS. The 1.5 mL of HBSS containing 60 μM LY CH Dipotassium Salt (FUJIFILM Wako) was added to the apical chamber, and 2.6 mL of HBSS was also added to the basolateral chamber. After 70-minute incubation at 37°C, the solution was

collected from the basolateral chamber. The LY fluorescent signal was measured with a fluorescence plate reader (TriStar LB 941) using 428-nm excitation and 535-nm emission filters. LY concentrations were calculated using the standard curve generated by serial dilution of LY.

Drug-Induced Hepatotoxicity Test

Human iPS-IECMs, which were cultured in the apical chamber, were cultured with 100 nM VD3 (Sigma-Aldrich) for 21 days and 20 μM RIF (FUJIFILM Wako) for 2 days. After the CYP3A4 induction, the apical chamber was moved onto the basolateral chamber, which contained 1-aminobenzotriazole (a CYP inhibitor)-treated human iPSC–derived hepatocyte-like cells. Hepatocyte-like cells were generated as described in our previous study.[30,31] To inhibit CYP activities in the hepatocyte-like cells, these cells were treated with 200-μM 1-aminobenzotriazole for 48 hours before the co-culture. Human iPS-IECMs and hepatocyte-like cells were co-cultured with amiodarone hydrochloride–containing medium (LKT Laboratories, Minneapolis, USA) for 48 hours. Then, the cell viability was assessed by using a WST-8 assay kit (Dojindo, Kumamoto, JAPAN). The cell viability of nontreated cells was taken as 100 in Figure 7*A*.

Human iPS-IECMs, which were cultured in the apical chamber, were cultured with 12.5-μM 6′,7′-dihydroxybergamottin (Sigma-Aldrich) and 1.98-μM bergamottin (Sigma-Aldrich), which are both main components of GFJ, for 48 hours. After the CYP3A4 inhibition, the apical chamber was moved onto the basolateral chamber, which contained human iPSC–derived hepatocyte-like cells. Human iPS-IECMs and hepatocyte-like cells were co-cultured with amiodarone hydrochloride–containing medium for 48 hours. Then, the cell viability was assessed by using a WST-8 assay kit (Dojindo). The cell viability of nontreated cells was taken as 100 in Figure 7*B*.

Determination of Fg Value

Human iPS-IECMs, which were cultured on the cell culture inserts, were preincubated with HBSS adjusted to pH 7.4 with 10-mM HEPES for 10 minutes at 37°C. The 1.5 mL of HBSS containing 3-μM MDZ was added to the apical chamber, and 2.6 mL of HBSS containing 0.1% DMSO was also added to the basolateral chamber. After 60-minute incubation at 37°C, the solution was collected from the basolateral or apical chamber. In addition, human iPS-IECMs were collected at the same time after twice washing with 1mL HBSS. All samples were mixed with internal standard (50-ng/mL candesartan)–containing acetonitrile/ethanol (7:3, v/v). The amount of MDZ and 1′-OH MDZ was measured using UPLC-MS/MS as we described above. The amounts of 1′-OH MDZ found in the apical, basolateral, and cell compartments were summed and entered into following equation, along with the amount of MDZ in the basolateral and cell compartments, to calculate *Fg* value. When apical dosing concentrations of MDZ were relatively low (eg, 3 μM), it is previously reported that 4′-OH MDZ did not contribute significantly to total metabolite formation and it was not included in the calculation of *Fg*. It is known that *Fg* values of VD3-treated Caco-2 cells and human in vivo are 0.86 and 0.57, respectively.[32–34]

$$Fg\ (\%) = \mathrm{MDZ}_{(\mathrm{basolateral+cell})} \Big/ \Big[\mathrm{MDZ}_{(\mathrm{basolateral+cell})} + \sum (1' - \mathrm{OH\ MDZ})\Big]$$

Membrane Permeability of Test Compounds

Human iPS-IECMs, which were cultured on the cell culture inserts, were preincubated with HBSS adjusted to pH 7.4 with 10-mM HEPES for 10 minutes at 37°C. The 1.5 mL of HBSS containing 1-μM antipyrine, metoprolol, fexofenadine, atenolol, and pravastatin was added to the apical chamber, and 2.6 mL of HBSS containing 0.1% DMSO was also added to the basolateral chamber. Antipyrine, metoprolol, fexofenadine, atenolol, and pravastatin were purchased from Sigma-Aldrich. After 30-, 60-, 90-, and 120-minute incubation at 37°C, the solution was collected from the basolateral chamber. Antipyrine, metoprolol, fexofenadine, atenolol, and pravastatin concentration was measured by UPLC-MS/MS. The *Fa* values of antipyrine, metoprolol, fexofenadine, atenolol, and pravastatin were cited from previous studies.[35–37]

Ad Vectors

Ad vectors were constructed by an improved in vitro ligation method.[38,39] The human CDX1, CDX2, KLF5, and SOX9 genes (accession number NM_001804.2, NM_001265.5, NM_001286818.1, and NM_000346.3) was amplified by PCR. The human CDX1, CDX2, KLF5, and SOX9 genes were inserted into pHMCA5,[40] which contains the CMV enhancer/chicken beta actin promoter, resulting in pHMCA5-CDX1, pHMCA5-CDX2, pHMCA5-KLF5, and pHMCA5-SOX9, respectively. The pHMCA5-CDX1, pHMCA5-CDX2, pHMCA5-KLF5, and pHMCA5-SOX9 were digested with *I-Ce*uI/*PI-Sc*eI and ligated into *I-Ce*uI/*PI-Sc*eI–digested pAdHM41-K7,[19] resulting in pAd-CDX1, pAd-CDX2, pAd-KLF5, and pAd-SOX9, respectively. The LacZ-, FOXA2-, and SOX17-expressing Ad vectors (Ad-LacZ, Ad-FOXA2, and Ad-SOX17, respectively) were constructed previously.[41,42] All of the Ad vectors contain a stretch of lysine residue (K7) peptides in the C-terminal region of the fiber knob for more efficient transduction of human pluripotent stem cells and their derivatives, in which the transfection efficiency was almost 100%, and were purified as described previously.[42–44] The VP titer was determined by using a spectrophotometric method.[45]

RNA Preparation and Microarray Analysis

Total RNA was isolated from undifferentiated human iPSCs, human iPS (YOW-iPS) cell derivatives, and Caco-2 cells using Trizol LS (Thermo Fisher Scientific) and an RNeasy mini kit (Qiagen) following the manufacturer's instructions. cRNA amplification, labeling, hybridization, and analysis were performed at TAKARA BIO INC. using SurePrint G3 Human Gene Expression 8x60K v3 (Agilent Technologies, Palo Alto, USA).

References

1. Watkins PB, Wrighton S, Schuetz E, Molowa DT, Guzelian P. Identification of glucocorticoid-inducible cytochromes P-450 in the intestinal mucosa of rats and man. J Clin Invest 1987;80:1029–1036.
2. Paine MF, Khalighi M, Fisher JM, Shen DD, Kunze KL, Marsh CL, Perkins JD, Thummel KE. Characterization of interintestinal and intraintestinal variations in human CYP3A-dependent metabolism. J Pharmacol Exp Ther 1997;283:1552–1562.
3. Thummel KE, Kunze KL, Shen DD. Enzyme-catalyzed processes of first-pass hepatic and intestinal drug extraction. Adv Drug Deliv Rev 1997;27:99–127.
4. Fromm MF, Busse D, Kroemer HK, Eichelbaum M. Differential induction of prehepatic and hepatic metabolism of verapamil by rifampin. Hepatology 1996;24:796–801.
5. Gomez DY, Wacher VJ, Tomlanovich SJ, Hebert MF, Benet LZ. The effects of ketoconazole on the intestinal metabolism and bioavailability of cyclosporine. Clin Pharm Ther 1995;58:15–19.
6. Martignoni M, Groothuis GM, de Kanter R. Species differences between mouse, rat, dog, monkey and human CYP-mediated drug metabolism, inhibition and induction. Expert Opin Drug Metab Toxicol 2006;2:875–894.
7. Balimane PV, Chong S. Cell culture-based models for intestinal permeability: a critique. Drug Discov Today 2005;10:335–343.
8. Lennernäs H, Nylander S, Ungell A-L. Jejunal permeability: a comparison between the Ussing chamber technique and the single-pass perfusion in humans. Pharm Res 1997;14:667–671.
9. Ozawa T, Takayama K, Okamoto R, Negoro R, Sakurai F, Tachibana M, Kawabata K, Mizuguchi H. Generation of enterocyte-like cells from human induced pluripotent stem cells for drug absorption and metabolism studies in human small intestine. Sci Rep 2015;5:16479.
10. Kauffman AL, Gyurdieva AV, Mabus JR, Ferguson C, Yan Z, Hornby PJ. Alternative functional in vitro models of human intestinal epithelia. Front Pharmacol 2013;4:79.
11. Spence JR, Mayhew CN, Rankin SA, Kuhar MF, Vallance JE, Tolle K, Hoskins EE, Kalinichenko VV, Wells SI, Zorn AM. Directed differentiation of human pluripotent stem cells into intestinal tissue in vitro. Nature 2011;470:105–109.
12. Yin J, Tse C-M, Avula LR, Singh V, Foulke-Abel J, de Jonge HR, Donowitz M. Molecular basis and differentiation-associated alterations of anion secretion in human duodenal enteroid monolayers. Cell Mol Gastroenterol Hepatol 2018;5:591–609.
13. Miura S, Suzuki A. Generation of mouse and human organoid-forming intestinal progenitor cells by direct lineage reprogramming. Cell Stem Cell 2017;21:456–471.e5.
14. Zhang R-R, Koido M, Tadokoro T, Ouchi R, Matsuno T, Ueno Y, Sekine K, Takebe T, Taniguchi H. Human iPSC-derived posterior gut progenitors are expandable and capable of forming gut and liver organoids. Stem Cell Reports 2018;10:780–793.
15. Ogaki S, Morooka M, Otera K, Kume S. A cost-effective system for differentiation of intestinal epithelium from human induced pluripotent stem cells. Sci Rep 2015;5:17297.
16. Negoro R, Takayama K, Nagamoto Y, Sakurai F, Tachibana M, Mizuguchi H. Modeling of drug-mediated CYP3A4 induction by using human iPS cell-derived enterocyte-like cells. Biochem Biophys Res Commun 2016;472:631–636.
17. Iwao T, Toyota M, Miyagawa Y, Okita H, Kiyokawa N, Akutsu H, Umezawa A, Nagata K, Matsunaga T. Differentiation of human induced pluripotent stem cells into functional enterocyte-like cells using a simple method. Drug Metab Pharmacokinet 2014;29:44–51.
18. Negoro R, Takayama K, Kawai K, Harada K, Sakurai F, Hirata K, Mizuguchi HJ. Efficient generation of small intestinal epithelial-like cells from human iPSCs for drug absorption and metabolism studies. Stem Cell Reports 2018;11:1539–1550.
19. Koizumi N, Mizuguchi H, Utoguchi N, Watanabe Y, Hayakawa T. Generation of fiber-modified adenovirus vectors containing heterologous peptides in both the HI loop and C terminus of the fiber knob. J Gene Med 2003;5:267–276.
20. Takayama K, Inamura M, Kawabata K, Katayama K, Higuchi M, Tashiro K, Nonaka A, Sakurai F, Hayakawa T, Furue MK. Efficient generation of functional hepatocytes from human embryonic stem cells and induced pluripotent stem cells by HNF4α transduction. Mol Therapy 2012;20:127–137.
21. Takayama K, Inamura M, Kawabata K, Sugawara M, Kikuchi K, Higuchi M, Nagamoto Y, Watanabe H, Tashiro K, Sakurai F. Generation of metabolically functioning hepatocytes from human pluripotent stem cells by FOXA2 and HNF1α transduction. J Hepatol 2012;57:628–636.
22. Mason JW. Amiodarone. N Engl J Med 1987;316:455–466.
23. Zahno A, Brecht K, Morand R, Maseneni S, Török M, Lindinger PW, Krähenbühl S. The role of CYP3A4 in amiodarone-associated toxicity on HepG2 cells. Biochem Pharm 2011;81:432–441.
24. Stringer EJ, Duluc I, Saandi T, Davidson I, Bialecka M, Sato T, Barker N, Clevers H, Pritchard CA, Winton DJ. Cdx2 determines the fate of postnatal intestinal endoderm. Development 2012;139:465–474.
25. Gao N, White P, Kaestner KH. Establishment of intestinal identity and epithelial-mesenchymal signaling by Cdx2. Dev Cell 2009;16:588–599.
26. Silberg DG, Sullivan J, Kang E, Swain GP, Moffett J, Sund NJ, Sackett SD, Kaestner KHJG. Cdx2 ectopic expression induces gastric intestinal metaplasia in transgenic mice. Gastroenterology 2002;122:689–696.
27. Yan L-H, Wei W-Y, Cao W-L, Zhang X-S, Xie Y-B, Xiao Q. Overexpression of CDX2 in gastric cancer cells promotes the development of multidrug resistance. Am J Cancer Res 2015;5:321–332.
28. Kasendra M, Tovaglieri A, Sontheimer-Phelps A, Jalili-Firoozinezhad S, Bein A, Chalkiadaki A, Scholl W, Zhang C, Rickner H, Richmond CA. Development of a

primary human small intestine-on-a-chip using biopsy-derived organoids. Sci Rep 2018;8:2871.
29. Jalili-Firoozinezhad S, Prantil-Baun R, Jiang A, Potla R, Mammoto T, Weaver JC, Ferrante TC, Kim HJ, Cabral JM, Levy O. Modeling radiation injury-induced cell death and countermeasure drug responses in a human gut-on-a-chip. Cell Death Dis 2018;9:223.
30. Takayama K, Morisaki Y, Kuno S, Nagamoto Y, Harada K, Furukawa N, Ohtaka M, Nishimura K, Imagawa K, Sakurai F. Prediction of interindividual differences in hepatic functions and drug sensitivity by using human iPS-derived hepatocytes. Proc Natl Acad Sci U S A 2014;111:16772–16777.
31. Takayama K, Akita N, Mimura N, Akahira R, Taniguchi Y, Ikeda M, Sakurai F, Ohara O, Morio T, Sekiguchi K. Generation of safe and therapeutically effective human induced pluripotent stem cell-derived hepatocyte-like cells for regenerative medicine. Hepatol Commun 2017;1:1058–1069.
32. Cummins CL, Jacobsen W, Christians U, Benet LZ. CYP3A4-transfected Caco-2 cells as a tool for understanding biochemical absorption barriers: studies with sirolimus and midazolam. J Pharmacol Exp Ther 2004;308:143–155.
33. Fahmi OA, Hurst S, Plowchalk D, Cook J, Guo F, Youdim K, Dickins M, Phipps A, Darekar A, Hyland R. Investigation of different algorithms for predicting clinical drug-drug interactions, based on the use of CYP3A4 in vitro data; predictions of compounds as precipitants of interaction. Drug Metab Dispos 2009;37:1658–1666.
34. Fisher JM, Wrighton SA, Watkins PB, Schmiedlin-Ren P, Calamia JC, Shen DD, Kunze KL, Thummel KE. First-pass midazolam metabolism catalyzed by 1α, 25-dihydroxy vitamin D3-modified Caco-2 cell monolayers. J Pharmacol Exp Ther 1999;289:1134–1142.
35. Sugano K, Takata N, Machida M, Saitoh K, Terada K. Prediction of passive intestinal absorption using bio-mimetic artificial membrane permeation assay and the paracellular pathway model. Int J Pharm 2002;241:241–251.
36. Skolnik S, Lin X, Wang J, Chen X-H, He T, Zhang B. Towards prediction of in vivo intestinal absorption using a 96-well Caco-2 assay. J Pharm Sci 2010;99:3246–3265.
37. Takenaka T, Harada N, Kuze J, Chiba M, Iwao T, Matsunaga T. Human small intestinal epithelial cells differentiated from adult intestinal stem cells as a novel system for predicting oral drug absorption in humans. Drug Metab Dispos 2014;42:1947–1954.
38. Mizuguchi H, Kay MA. Efficient construction of a recombinant adenovirus vector by an improved in vitro ligation method. Hum Gene Ther 1998;9:2577–2583.
39. Mizuguchi H, Kay MA. A simple method for constructing E1- and E1/E4-deleted recombinant adenoviral vectors. Hum Gene Ther 1999;10:2013–2017.
40. Kawabata K, Sakurai F, Yamaguchi T, Hayakawa T, Mizuguchi H. Efficient gene transfer into mouse embryonic stem cells with adenovirus vectors. Mol Ther 2005;12:547–554.
41. Tashiro K, Kawabata K, Sakurai H, Kurachi S, Sakurai F, Yamanishi K, Mizuguchi H. Efficient adenovirus vector-mediated PPAR gamma gene transfer into mouse embryoid bodies promotes adipocyte differentiation. J Gene Med 2008;10:498–507.
42. Takayama K, Inamura M, Kawabata K, Tashiro K, Katayama K, Sakurai F, Hayakawa T, Furue MK, Mizuguchi H. Efficient and directive generation of 2 distinct endoderm lineages from human ESCs and iPSCs by differentiation stage-specific SOX17 transduction. PLoS One 2011;6:e21780.
43. Tashiro K, Kawabata K, Inamura M, Takayama K, Furukawa N, Sakurai F, Katayama K, Hayakawa T, Furue MK, Mizuguchi H. Adenovirus vector-mediated efficient transduction into human embryonic and induced pluripotent stem cells. Cell Reprogram 2010;12:501–507.
44. Takayama K, Inamura M, Kawabata K, Katayama K, Higuchi M, Tashiro K, Nonaka A, Sakurai F, Hayakawa T, Furue MK, Mizuguchi H. Efficient generation of functional hepatocytes from human embryonic stem cells and induced pluripotent stem cells by HNF4alpha transduction. Mol Therapy 2012;20:127–137.
45. Maizel JV Jr, White DO, Scharff MD. The polypeptides of adenovirus. I. Evidence for multiple protein components in the virion and a comparison of types 2, 7A, and 12. Virology 1968;36:115–125.

Received September 23, 2018. Accepted June 12, 2019.

Correspondence
Address correspondence to: Kazuo Takayama, PhD, Laboratory of Biochemistry and Molecular Biology, Graduate School of Pharmaceutical Sciences, Osaka University, 1-6 Yamadaoka, Suita, Osaka 565-0871, Japan. e-mail: takayama@phs.osaka-u.ac.jp; fax: +81-6-6879-8187; or Hiroyuki Mizuguchi, PhD, Laboratory of Biochemistry and Molecular Biology, Graduate School of Pharmaceutical Sciences, Osaka University, 1-6 Yamadaoka, Suita, Osaka 565-0871, Japan. e-mail: mizuguch@phs.osaka-u.ac.jp; fax: +81-6-6879-8187.

Acknowledgments
The authors thank Ms Yasuko Hagihara, Ms Natsumi Mimura, and Ms Ayaka Sakamoto for their excellent technical support. They also thank Ms Miyako Maeda (GenoMembrane, Co, Ltd) for excellent technical support.

Author contributions
Designed research: KT, HM; acquisition of data: KT, RN, TY, TM; analysis and interpretation of data: KT, RN, TY, KK, MI, TM, NN, K. Harada, S. Ito, HY, YY, K. Hirata, S. Ishida, HM; statistical analysis: KT; and wrote manuscript: KT, HM.

Conflicts of interest
The authors disclose no conflicts

Funding
This research is supported by the grants from Japan Agency for Medical Research and development, AMED (16mk0104004h0303), Mochida Memorial Foundation for Medical and Pharmaceutical Research, Uehara Memorial Foundation, and JSPS KAKENHI Grant Number (18H05033, 18H05373). TY is supported by a Grant-in-aid for the Japan Society for the Promotion of Science Fellows.